Energy Efficiency Analysis of UAV-Assisted mmWave HetNets

***Abstract*—We study a multi-band heterogeneous network comprising aerial (UAV) small base stations and ground-based dual mode mmWave small cells within the coverage area of a microwave (μW) macro base station. We formulate a two-layer optimization framework to simultaneously find an efficient coverage radius of the UAVs and energy efficient radio resource management for the network, subject to minimum quality-of-service (QoS) and maximum transmission power constraints. The outer layer derives an optimal coverage radius/height for each UAV as a function of the maximum allowed path loss, whereas the inner layer formulates an optimization problem to maximize the system energy efficiency (EE). Our results demonstrate that at certain values of the target SINR τ introducing the UAVs doubles the EE. We also show that an increase in τ beyond an optimal EE point decreases the EE.**

I. Introduction

5G technologies will comprise a mix of network tiers of different sizes, transmission powers, backhaul connections, and radio access technologies [1]. The use of drone small cells or wireless aerial platforms has been proposed recently to improve network coverage and capacity [2]. Additionally, UAVs are expected to prove instrumental for public safety and disaster management [3]. We consider a heterogeneous network comprising a μW macro BS, ground-based dual-mode mmWave small BS (SBS), and aerial (UAV) BS, as illustrated in Figure 1. Related UAV work has largely dealt

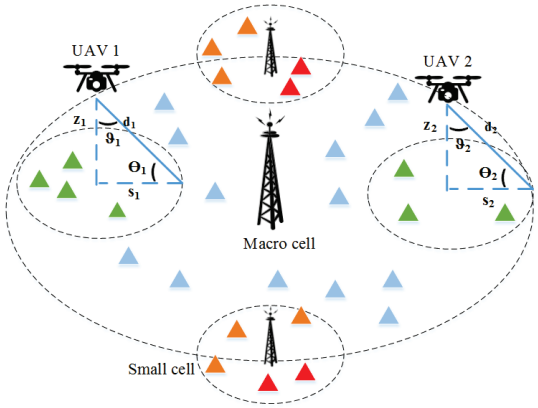

Fig. 1: The investigated system model.

with air-to-ground channel modeling, investigating line-of-sight (LoS) probability and path loss [4, 5]. We leverage the LoS probability expression from [6]. While promising, UAV BS present several operational challenges ranging from energy limitations and interference management to optimal 3D deployment. [7] determines the optimal UAV altitude to minimize transmitted power required to cover a target region. [8] extends this work by determining the optimal UAV locations given their corresponding cell boundaries are known. However, both studies do not consider ground-based small and macro cells existing simultaneously. [9] studies proactive deployment of cache-enabled UAVs for optimizing a given QoE metric, determining user-UAV associations, the optimal UAV locations, and the cached content.

Another feature of 5G networks is the use of mmWave and μW resources simultaneously. The utilization of mmWave technology has recently gained attention due to the higher available bandwidth (in the range of 1–2 GHz) and the possibility of larger antenna arrays due to the smaller wavelength of mmWave signals [10]. The authors in [11] present a novel scheduling framework for small cells operating in dual mode, i.e., in both mmWave and ultra high frequency (UHF) bands. We adopts a similar approach towards transmissions from the SBS, whereby the users in the small cell may utilize one of the two frequencies available at the mmWave band, depending on which one maximizes their respective rate. In contrast to related work [7, 12], we study for the first time the EE of a UAV-assisted multi-band HetNet, comprising ground based macro BS and dual-mode mmWave SBS, and derive an optimization framework to maximize it. We propose a joint subcarrier and power allocation scheme to maximize the system EE while satisfying a minimum QoS level for the users and a maximum power transmission constraint. To solve this radio resource management problem, we propose a two-layer framework, where in the the first phase, the EE of μW users is maximized, while in the second phase, the power consumption of the UAV tier is optimized to satisfy their users' minimum rate requirement and limit the maximum allowed interference from the UAV tier to the μW users.

The rest of this paper is organized as follows. Section II presents our system models, formulating the considered infrastructure and air-to-ground channels. Sections III-V formulate the power allocation mechanisms for the μW BS, the UAVs, and the SBS, respectively. In Section VI, we present our experimental results. Section VII concludes the paper.

II. System Model

The network comprises a macro cell BS, W SBS, and E UAV BS, with a total of M users distributed randomly in the region of interest. The macro cell BS is denoted as μW. Each UAV and the μW BS share $N_{\mu W}$ subcarriers, whereas each mmWave SBS w has two available mmWave bands $b \in \{H, L\}$ where H represents the higher mmWave band, which is noise limited, and L represents the lower mmWave band, which is interference limited. Each user is expected to achieve a minimum data rate $R_{\min}$. It should be noted that all BS in the three-tier hybrid HetNet operate independently to find their optimal transmission power in a distributed manner [13]. We assume that each subcarrier can be exclusively assigned to only one user within the same BS

of each tier k. We assume that user m associates to the tier k with the maximum biased received power $\Gamma_m^k = \frac{\beta_k P_k^{\max} G(\theta_k)}{\mathrm{PL}_m^k}$, where $P_k^{\max}$ is the maximum transmission power of tier k, β_k is the biasing factor of the tier $k \in \{\text{macro}, \text{UAV}, \text{mm}\}$, θ_k is the azimuthal angle of the BS beam alignment. Based on this user association scheme, user m can belong to one of the following three disjoint sets

$$m = \begin{cases} m_1, \text{if } m \text{ is served by } \mu\text{W or mmWave band } L \text{ tier}, \\ m_2, \text{if } m \text{ is served by UAV tier}, \\ m_3, \text{if } m \text{ is served by mmWave band } H \text{ tier}, \end{cases}$$

where m_1 denotes the users that aim to maximize their EE, m_2 denotes the users that aim to minimize their power consumption, and m_3 denotes the users that aim to maximize their data rate. The achievable rate of user m on subcarrier n associated with tier $l \in \{\text{macro, UAV}\}$ is

$$r_{m,n}^{(l)} = \Theta_l B_l \log_2(1 + \gamma_{m,n}^{(l)} \times p_{m,n}^{(l)}), \tag{1}$$

where Θ_l is the proportion of bandwidth allocated to each subcarrier by the associated BS of tier l, B_l indicates the total bandwidth available to the associated BS of tier l and $p_{m,n}^{(l)}$ indicates the power allocated to user m on the subcarrier n by associated BS of tier l.

The distance d between user m and its associated UAV e is

$$d = \sqrt{(x - x_e)^2 + (y - y_e)^2 + z_e^2}, \tag{2}$$

where x_e, y_e and z_e represent the x, y and z coordinates of a UAV e in a cartesian plane. The altitude of the UAV e is $z_e = s_e \tan(\theta_e)$, where s_e is the 2D distance of m from e and $\theta_e = \pi/2 - \vartheta$, for ϑ the UAV's half beamwidth angle. Similarly, the LoS probability between e and m is given as $P_{\text{LoS}} = 1/(1 + \mathrm{C} \cdot \exp[-\mathrm{Y}(\theta_e - \mathrm{C})])$ [6], where C and Y are constants dependent on the environment settings (rural, urban, dense urban, or others).

A. Dual Mode mmWave Small Cells

We consider that the SBS are using TDMA. The average achievable rate of user m on subcarrier n associated with the mmWave tier on band b across T time slots is,

$$r_{m,n}^{w,b} = \frac{1}{T} \sum_{t=1}^{T} \Theta_{w,b} B_{w,b} \log_2(1 + \gamma_{m,n_t}^{w,b} \times p_{m,n_t}^{w,b}), \tag{3}$$

where $\Theta_{w,b}$ is the bandwidth share allocated to each subcarrier on band b, $B_{w,b}$ indicates the total bandwidth available to the mmWave SBS on band b, and $p_{m,n_t}^{w,b}$ indicates the power allocated to user m on the subcarrier n_t at time slot t. Thus, the total achieved rate of user m associated with SBS w is $r_{m,n}^{w} = \sum_{b \in \{H,L\}} r_{m,n}^{w,b}$. Finally, the total data rate for user m, associated with either μW BS, UAV BS, or w SBS is

$$\overline{R_m} = \sum_{k \in \{l,w\}} \sum_{n=1}^{N_k} \sigma_{m,k} r_{m,n}^{(k)}, \tag{4}$$

where $\sigma_{m,k} = 1$, if m is associated with tier k and 0 otherwise, and N_k is the total number of subcarriers available to tier k.

We denote the total power consumed by user m as $\overline{P_m} = \sum_{k \in \{l,w\}} \sum_{n=1}^{N_k} \sigma_{m,k} p_{m,n}^{(k)}$. Then, we define the system EE as $\sum_{m=1}^{M} \overline{R_m} / (\sum_{m=1}^{M} \overline{P_m} + \sum_{k \in K} P_{\mathrm{C}_k})$, where P_{C_k} is the circuit power of tier k.

B. Determining the optimal altitude of a UAV

We determine UAV e's height above ground such that the maximum path loss experienced at transmission is limited to $\mathrm{PL}_{\max}$. We derive the latter as

$$\mathrm{PL}_{\max} = d^{\alpha^e} [P_{\text{LoS}}(10^{0.1 \times \eta_{\text{LoS}}}) + P_{\text{NLoS}}(10^{0.1 \times \eta_{\text{NLoS}}})], \tag{5}$$

where $P_{\text{NLoS}} = 1 - P_{\text{LoS}}$, $\eta_{\text{LoS/NLoS}}$ is the average additional loss in LoS and NLoS links relative to the free space propagation loss, d is the distance of the farthest user, and α^e is the path loss exponent for UAV e.

Subsequently, we derive z_e from $\mathrm{PL}_{\max}$ as

$$z_e = \cos(\vartheta) \frac{\mathrm{PL}_{\max}}{[P_{\text{LoS}}(10^{0.1 \times \eta_{\text{LoS}}}) + P_{\text{NLoS}}(10^{0.1 \times \eta_{\text{NLoS}}})]}. \tag{6}$$

III. Power Allocation Mechanism for μW BS

Our objective here is to simultaneously optimize the achievable rate and EE of all users associated with the μW BS subject to a maximum transmission power constraint and minimum required QoS level. The joint optimization is equivalent to maximizing the sum rate and minimizing the total power consumption for the users. We formulate it as a multi-objective problem which we then transform into a single objective optimization using the weighted sum method by normalizing the two objectives by R_{norm} and P_{norm}, respectively, to ensure a consistent comparison as shown below:

$$\max_{\mathbf{p}} \phi \frac{\sum_{m \in M_{\mu W}} \sum_{n \in N_{\mu W}} \sigma_{m,n} r_{m,n}^{(\mu W)}}{R_{\text{norm}}} - (1 - \phi) \frac{P}{P_{\text{norm}}}, \tag{7}$$

$$\text{subject to: } \sum_{m \in M_{\mu W}} \sum_{n \in N_{\mu W}} p_{m,n}^{(\mu W)} \leq P_{\mu W}^{\max},$$

$$R_m \geq R_{\min}, \forall m, \; p_{m,n}^{(\mu W)} \geq 0, \sigma_{m,n} \in [0,1], \forall m, n,$$

where $M_{\mu W}$ represents the total number of users associated with μW BS such that $\sigma_{m,\mu W} = 1$ and $N_{\mu W}$ represents the total number of available subcarriers to this BS. We note that while the user association has already been done beforehand, we use the subscript μW to improve the readability here. In addition, P_{norm} is the maximum transmit power of the BS, R_{norm} is the maximum achievable rate corresponding to P_{norm}, and $P = \sum_{m,n} p_{m,n}^{(\mu W)}$. Since user m can share at most one subcarrier with another user associated with a UAV BS, we can decompose (7) into (i) a power allocation problem for users associated with the μW BS and a UAV, and (ii) a subcarrier allocation problem for the users associated with the μW BS. We formulate the first problem as

$$\max_{\mathbf{p}} \phi \frac{\sum_{m \in M_{\mu W}} \sum_{n \in N_{\mu W}} r_{m,n}^{(\mu W)}}{R_{\text{norm}}} - (1 - \phi) \frac{P}{P_{\text{norm}}}, \tag{8}$$

subject to the first three constraints in (7).

We note that when ϕ =1, (8) transforms into rate maximization, while for ϕ =0 it transforms into power minimization. Moreover, for $\phi = \phi_{\text{EE}} \in [0,1]$, it transforms into EE maximization. We write the Lagrangian function for (8) as

$$T(\mathbf{p},\boldsymbol{\mu},\boldsymbol{\varphi}) = \frac{\phi}{R_{\text{norm}}}\sum_{m,n} r_{m,n}^{(\mu W)} - \frac{(1-\phi)}{P_{\text{norm}}}P + \mu\left(P_{\mu W}^{\max} - \sum_{m,n} p_{m,n}^{(\mu W)}\right) + \sum_{m\in M_{\mu W}} \varphi_m(R_m - R_{\min}),$$

where $P_{\mu W}^{\max}$ is the maximum transmit power of the μW BS.

The optimal value $p_{m,n}^{(\mu W)}$ can then be computed as

$$p_{m,n}^{(\mu W)} = \left[\frac{\left(\frac{\phi}{R_{\text{norm}}} + \varphi_m\right)\Theta_{\mu W} B_{\mu W}}{\left(\mu + \frac{1-\phi}{P_{\text{norm}}}\right)(\ln 2)} - \frac{1}{\gamma_{m,n}^{(\mu W)}}\right]^+, \quad (9)$$

where μ and φ_m are the Lagrangian multipliers associated with the first two constraints in (7), which we update using a sub-gradient method as follows:

$$\mu_{\mu W}(j+1) = \left[\mu_{\mu W}(j) - s_1\left(P_{\mu W}^{\max} - \sum_{m=1}^{M_{\mu W}}\sum_{n=1}^{N_{\mu W}} p_{m,n}^{(\mu W)}\right)\right]^+,$$

$$\varphi_m(j+1) = \left[\varphi_m(j) - s_2\left(R_m - R_{\min}\right)\right]^+,$$

where $\left[x\right]^+ = \max(0,x)$. Algorithm 1 provides an algorithmic description of the formulated power allocation mechanism. Using $p_{m,n}^*$ as the optimal power allocation solution to

Algorithm 1 Power allocation for users of μW BS

1: Set $j = 0$ and $j_{\max} = 10^4$, initialize $p_{m,n}^{(\mu W)} = 10^{-6}$, $\varphi_m = 10^{-2}$, $\forall m$ and $\mu_{\mu W} = 10^{-2}$.
2: **while** φ_m and $\mu_{\mu W}$ have not converged or $j < j_{\max}$ **do**
3: Compute $p_{m,n}^{(\mu W)}$ using (23)
4: Update $\mu_{\mu W}(j+1)$ and $\varphi_m(j+1)$
5: **end while**
6: End

(8), for the users associated with the μW BS, we model the subcarrier allocation problem as

$$\max_{\sigma_{m,n}} \sum_{m,n} \sigma_{m,n} p_{m,n}^*, \text{ s.t. } \sigma_{m,n} \in [0,1], \forall m,n. \quad (10)$$

We solve (10) using the Hungarian method [14].

IV. Power Allocation Mechanism for UAVs

To guarantee QoS to users associated with the μW BS, we impose a maximum interference threshold constraint I_t such that the total cross-tier interference caused by the UAV to the user associated with the μW BS and sharing the same subcarrier should always be less than or equal to I_t. The transmission power on a reused subcarrier by the UAV should be chosen such that the μW BS users can satisfy their minimum rate requirement. We calculate this power from

$$\log_2\left(1 + \frac{p_{m,n}^{(\mu W)}|\mathrm{h}_{m,n}^{(\mu W)}|^2}{\left(\sigma^2 + \frac{p_{m,n}^e}{\mathrm{PL}_m^e}|\mathrm{h}_{m,n}^{(e)}|^2\right)\mathrm{PL}_m^{\text{macro}}}\right) \geq R_{\min},$$

$$\Rightarrow p_{m,n}^e \leq \frac{\mathrm{PL}_m^e}{|\mathrm{h}_{m,n}^{(e)}|^2}\left(\frac{p_{m,n}^{(\mu W)}|\mathrm{h}_{m,n}^{(\mu W)}|^2}{(2^{R_{\min}}-1)\mathrm{PL}_m^{\text{macro}}} - \sigma^2\right),$$

where $p_{m,n}^e$ is the transmission power of UAV e to user $m \in M_e$ on subcarrier n, which it shares with μW BS user $m \in M_{\mu W}$, $p_{m,n}^{(\mu W)}$ is the transmission power of the μW BS at the given subcarrier n to user $m \in M_{\mu W}$, PL_m^e is the path loss between UAV e and user $m \in M_e$, and $R_{\min}$ is the user minimum rate requirement.

Similarly, the transmission power of UAV e to user $m \in M_e$ on subcarrier n based on the predetermined interference threshold I_t can be computed as $\overline{p}_{m,n}^e \leq \frac{I_t\,\mathrm{PL}_m^e}{|\mathrm{h}_{m,n}^{(e)}|^2}$, where PL_m^e is the path loss experienced between UAV e and the user $m \in M_{\mu W}$ sharing the same subcarrier n.

Finally, the minimum transmission power that UAV e needs to use to meet the minimum rate requirement is

$$p_{m,n}^{e,\min} = \frac{\mathrm{PL}_m^e}{|\mathrm{h}_{m,n}^{(e)}|^2}\left(2^{R_{\min}}-1\right)\left(\sigma^2 + \frac{p_{m,n}^{(\mu W)}|\mathrm{h}_{m,n}^{(e)}|^2}{\mathrm{PL}_m^e}\right), \quad (11)$$

where PL_m^e is the path loss between UAV e and its associated user $m \in M_e$. Hence, the final constrained transmission power of UAV e to user m on subcarrier n is,

$$p_{m,n}^{e\,\text{opt}} = \begin{cases} \min\left(\overline{p}_{m,n}^e, \max\left(p_{m,n}^e, p_{m,n}^{e,\min}\right)\right), & \text{if} \Lambda \geq p_{m,n}^{e,\min}, \\ \text{Infeasible}, & \text{otherwise}, \end{cases}$$

where $\Lambda = \min\left(p_{m,n}^e, \overline{p}_{m,n}^e\right)$.

V. Power/Subcarrier Allocation for mmWave SBS

The SBS have the flexibility to serve their users on one of the available two mmWave bands $\{L, H\}$. As noted earlier, band H is assumed to be noise limited whereas the lower mmWave band L is assumed to be interference limited considering the co-tier interference among the SBS operating on this band. For band H, each subcarrier $n \in N_{w,H}$ is allocated transmission power $p_{m,n}^{w,H} = P_w^{\max}/N_{w,H}$, where $P_w^{\max}$ is the maximum transmit power of SBS w and $N_{w,H}$ is the total number of subcarriers available at SBS w on band H.

As the users served by SBS w on the lower band L experience co-tier interference from the neighbouring mmWave SBS, there is a need for efficient power control. Similarly to the mechanism described in Section III, the transmission power of SBS w operating on band L to user m on subcarrier $n \in N_{w,L}$ can be computed as

$$p_{m,n}^{w,L} = \left[\frac{\left(\frac{\phi}{R_{\text{norm}}} + \varphi_m\right)\Theta_{w,L} B_{w,L}}{\left(\mu_w + \frac{1-\phi}{P_{\text{norm}}}\right)(\ln 2)} - \frac{1}{\gamma_{m,n}^{(w)}}\right]^+, \forall m \in M_w, \forall n \in N_w.$$

Subcarrier pairing in the small cells operating on band H (noise limited regime) in TDMA is performed so as to allocate T combinations of subcarriers to each user which maximize their average achieved rate across T time slots. On the other hand, the small cells operating on band L (interference limited regime) allocate T combinations of subcarriers to each user to maximize their average achieved EE across T time slots. We omit here the detailed procedure for subcarrier pairing in dual-mode mmWave small cells in TDMA, to conserve space.

VI. Performance Evaluation

In our experiments, we consider a hybrid cellular network comprising one μW BS coexisting with three dual mode mmWave SBS ($W = 3$) and two UAV ($E = 2$) operating in the μW band. We consider 50 users uniformly distributed in a square geographical area 1 km $\times$ 1 km. The mmWave SBS are randomly deployed on the macro cell edge to cater to cell edge users. We consider a 2 GHz carrier frequency for both μW and UAVs whereas the carrier frequencies for small cells operating on the mmWave bands L and H are 28 GHz and 73 GHz. The bandwidth of both μW BS and UAVs are 20 MHz whereas the bandwidth of small cells operating on the mmWave bands L and H are 1 GHz and 2 GHz.

The maximum transmission power of μW BS, UAVs, and SBS are 46 dBm, 30 dBm, and 30 dBm. The total number of subcarriers available to each tier k is 128. The path loss exponent for the ground user-UAV link is 2 while that for μW BSs is 3. The LoS and NLoS pathloss exponents for mmWave small cells are 2 and 3.3[10]. The minimum rate requirement is set to 3 b/s/Hz unless otherwise stated. The thermal noise is assumed to be -174 dBm/Hz. The half power beamwidth angle for mmWave small cell is 10° [10] and the shadowing in μW BS or UAVs are considered to be 4 dB whereas the shadowing in mmWave small cells are 5.2 dB and 7.2 dB are LoS and NLoS links[15]. All statistical results are calculated over various channel conditions and user locations averaged by 10^3 *Monte Carlo* iterations.

Figure 2 depicts the number of users associated with the UAV tier for increasing β_{UAV} on the basis of biased received power using Γ_m^k and biased SINR. The six graphs in the figure represent various biasing scenarios for the SBS and the μW BS. When the biasing factors for both the mmWave SBS and the μW BS are 0 dB, it yields the greatest number of users associated with the UAV tier, irrespective of whether the association is done on the basis of biased received power or biased SINR. In fact, for the case when biasing is performed based on received power, increasing β_{UAV} from 10 dB to 15 dB causes an increase by approximately 67% in the number of users associated with the UAV tier. The graphs representing the cases when both the SBS and the UAV have non-zero biasing factors show a similar increasing trend. However, the cumulative number of users associated with the UAV tier remains lower than that for the previous case, as a greater number of users are now associated with the mmWave tier. As the maximum transmission power of the μW BS is the highest among all the tiers, therefore, introducing a non-zero

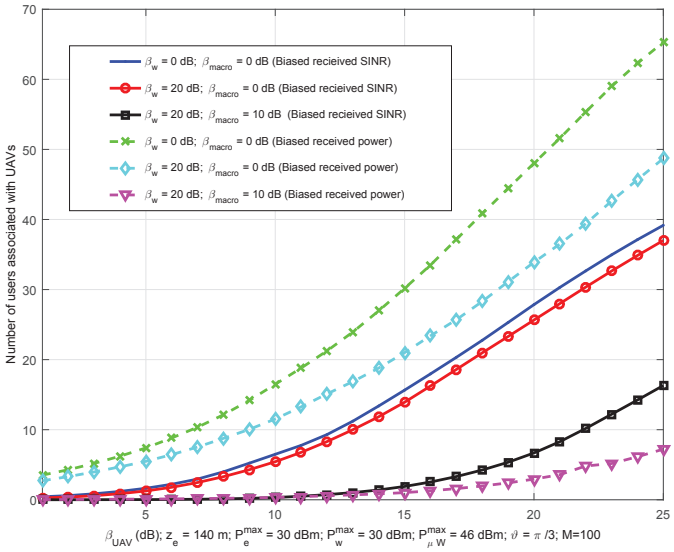

Fig. 2: User association for the UAV tier versus β_{UAV} based on biased received power and SINR.

biasing factor β_{macro} causes a sharp decline in the number of users associated with the UAV tier irrespective of the type of user association. The figure shows that at $\beta_{\text{UAV}} = 25$ dB, there is a nearly 84% decrease in the number of users utilizing the UAV tier when $\beta_{\text{UAV}} = 10$ dB, relative to when only the SBS biasing factor is taken to be non-zero.

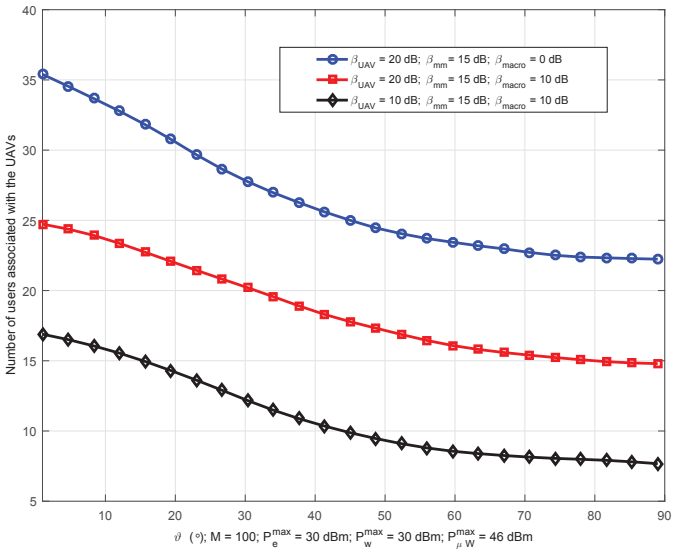

Fig. 3: User association for the UAV tier versus the half power beamwidth angle of the UAV.

The impact of the half power beam-width angle of the UAV, ϑ, on the number of users associated with the UAV tier is shown in Figure 3. User association is done on the basis of biased received power. All three curves demonstrate a general decrease with an increase in ϑ. This is due to the fact that an increase in ϑ causes a decrease in the elevation angle, θ_e, resulting in a small coverage radius s_e. Consequently, P_{LoS} in (8) decreases, which in turn causes an increased

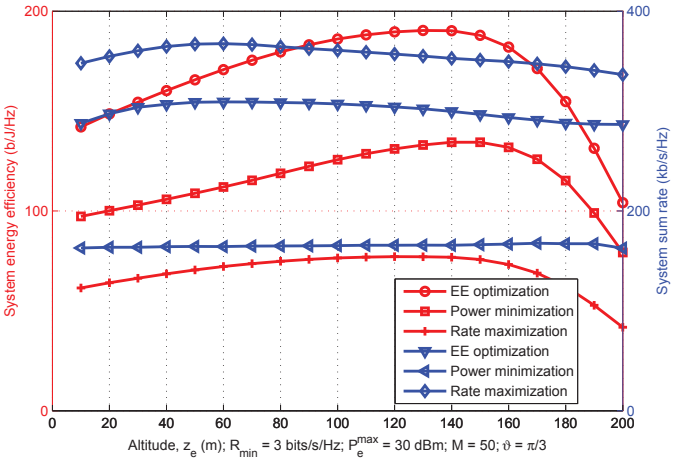

Fig. 4: System sum rate and system EE versus UAV altitude z_e.

path loss, PL_m^e, determined by (10). This increased path loss experienced by transmissions reduces association with the UAV tier. Additionally, of the three graphs in Figure 3, the one representing the scenario with the highest β_{UAV} and lowest β_{macro} clearly outperforms the other two. For instance, the number of users associated with the UAV tier in the case involving a β_{macro} of 0 dB at $\vartheta_{\text{UAV}} = 89°$ is nearly three times that of the scenario with $\beta_{\text{UAV}} = \beta_{\text{macro}} = 18$ dB.

Figure 4 describes the system sum rate and the system EE versus UAV altitude z_e, for all power allocation mechanisms. The graphs for system EE demonstrate that our EE maximization approach outperforms the power minimization and rate maximization power allocation mechanisms. It is also obvious that the system EE reaches a maximum point at $z_e = 140$m, which corresponds to PL_{max}=68.8 dB. Beyond this altitude, the system EE begins to decrease. In fact, the system EE at $z_e =$ 140 m, using the EE maximization approach is 35% greater in comparison to $z_e = 10$ m. Meanwhile, the system sum rate for the EE maximization approach reaches a maximum point when z_e = 50 m. It is shown that at higher UAV altitudes, while P_{LoS} increases, PL_m^e also increases due to an increased UAV-user distance. As a result of this all other simulations results are performed at $z_e = 140$m.

Figure 5 describes the system EE with or without the UAV tier, versus $\tau = 2^{R_{\text{min}}} - 1$. It is evident for the EE maximization approach that at τ = 0 dB, the system EE with a UAV tier is almost two times greater. Similarly, for the other two considered power allocation approaches, the advantages of including the UAV tier are quite evident from Figure 5.

Figure 6 depicts the system sum rate versus τ with and without the UAV tier, versus τ. The maximum achievable sum rate using the rate maximization approach in the presence of the UAV tier is approximately 13% greater. The results for the other power allocation approaches are also higher when the system includes the UAV tier. For instance, at τ = 20 dB, the achievable sum rate for the power minimization approach is approximately 10% greater.

The variation in system EE and system sum rate for all power allocation approaches versus increasing τ are examined in Figure 7. The EE maximization approach outperforms the power minimization and rate maximization approaches in terms of system EE, expectedly. At τ = -20 dB, the system EE for the power minimization approach is approximately 88% lower. However, an increase in τ subsequently results in an increase in the system EE for this approach and reaches a maximum point at $\tau = 0$ dB. The achievable system EE for the rate maximization approach remains constant irrespective of the values of τ. Additionally, as τ takes higher values, greater transmission power is required to achieve the minimum required QoS level, which causes a decrease in the system EE shown by the EE maximization and power minimization approaches. The rate maximization approach achieves the highest sum rate for the considered values of τ being investigated, as expected. At $\tau = 30$ dB, the achievable system sum rate for the EE maximization and power minimization approaches is approximately equal to the achieved sum rate for the rate maximization approach.

VII. Conclusion

We designed an efficient radio resource management optimization framework for a multi-tier multi-band mmWave cellular network integrating UAV-based aerial small cells for enhanced coverage/throughput. We analyzed the system EE and system sum rate, along with other metrics, of this setting, where a varying number of users could be associated with the UAV tier depending on the biasing factors of all three network tiers. Our results demonstrate that including a UAV tier in the network can nearly double the system EE at certain target SINR values. Furthermore, we showed that the system EE increases with an increase in UAV altitude and after an optimal UAV altitude, it starts decreasing. Our results show that our proposed approach outperforms traditional schemes aimed at maximizing the system sum rate or minimizing the system power consumption.

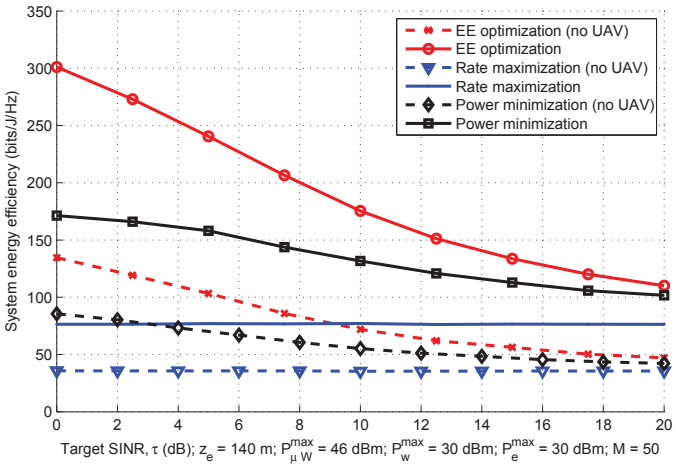

Fig. 5: System EE versus target SINR τ, both with and without the UAV tier.

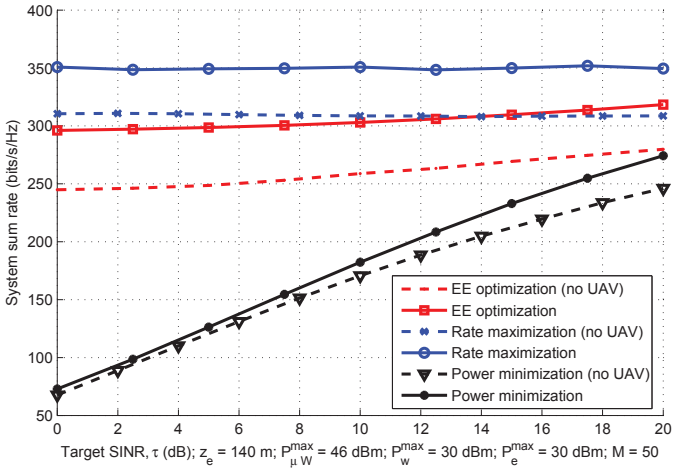

Fig. 6: System sum rate versus target SINR τ, with and without UAVs.

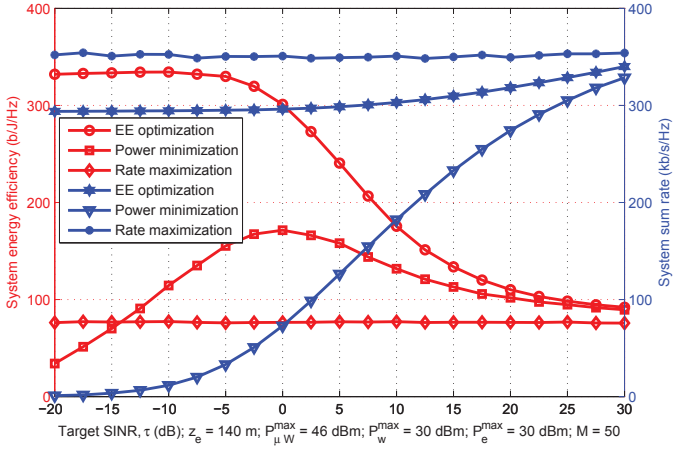

Fig. 7: System sum rate and system EE versus target SINR, τ.

REFERENCES

[1] E. Hossain, et al., "Evolution toward 5G multitier cellular wireless networks: An interference management perspective," *in Wireless Commun.*, vol. 21, no. 3, pp. 118-127, 2014.

[2] R. Yaliniz, A. El-Keyi, and H. Yanikomeroglu, "Efficient 3-D placement of an aerial base station in next generation cellular networks," in *Proc. of IEEE International Conference on Communications (ICC)*, May 2016.

[3] I. Bucaille, S. Hethuin, A. Munari, R. Hermenier, T. Rasheed, and S. Allsopp, "Rapidly deployable network for tactical applications: Aerial base station with opportunistic links for unattended and temporary events absolute example," *in Proc. of IEEE Military Communications Conference*, San Diego, CA, USA, Nov. 2013.

[4] A. Hourani, S. Kandeepan, and A. Jamalipour, "Modeling air-to-ground path loss for low altitude platforms in urban environments," *in Proc. of IEEE Global Communications Conference (GLOBECOM)*, USA, 2014.

[5] Q. Feng, J. McGeehan, E. K. Tameh, and A. R. Nix, "Path loss models for air-to-ground radio channels in urban environments," *in Proc. of IEEE Vehicular Technology Conference (VTC)*, Australia, 2006.

[6] A. Al-Hourani, S. Kandeepan, and S. Lardner, "Optimal LAP altitude for maximum coverage," *in IEEE Commun. Lett.*, vol. 3, no. 6, pp. 569–572, 2014.

[7] M. Mozaffari, W. Saad, M. Bennis, and M. Debbah, "Drone Small Cells in the Clouds: Design, Deployment and Performance Analysis," in *Proc. of the IEEE Global Communications Conference (GLOBECOM), Wireless Networks Symposium*, USA, Dec. 2015.

[8] M. Mozaffari, W. Saad, M. Bennis, and M. Debbah, "Optimal Transport Theory for Power-Efficient Deployment of Unmanned Aerial Vehicles," *in Proc. of the IEEE International Conference on Communications (ICC), Wireless Communications Symposium*, Malaysia, May 2016.

[9] M. Chen, M. Mozaffari, W. Saad, C. Yin, M. Debbah, C. Hong, "Caching in the sky: proactive deployment of cache-enabled unmanned aerial vehicles for optimized quality-of-experience," *arXiv:1610.01585 [cs.IT]*, 2016.

[10] S. Singh, M. Kulkarni, A. Ghosh and J. Andrews, "Tractable model for rate in self-backhauled millimeter wave cellular networks," *in IEEE J. Sel. Areas Commun.*, vol. 33, no. 10, pp. 2196-2211, Oct. 2015.

[11] O. Semiari, W. Saad and M. Bennis, "Joint millimeter wave and microwave resources allocation in cellular networks with dual-mode base stations," *arXiv:1606.08971*, 2016.

[12] V. Sharma, M. Bennis and R. Kumar, "UAV-Assisted heterogeneous networks for capacity enhancement," *in IEEE Commun. Lett.*, vol. 20, no. 6, pp. 1207 – 1210, 2016.

[13] N. Abuzainab and W. Saad, "Cloud radio access meets heterogeneous small cell networks: A cognitive hierarchy perspective," arXiv:1606.04198v1 [cs.IT], Jun. 2016.

[14] H. Kuhn, "The Hungarian method for the assignment problem," *Naval Research Logistics Quarterly 2*, pp. 83-97, 1955.

[15] T. Bai and R. Heath Jr., "Coverage and rate analysis for millimeter wave cellular networks," *arXiv:1402.6430*, 2014.